The effects of turbulence on cavitation inception

I. Anton
Technical University, Faculty of Mechanics
Department of Fluid Machinery
Bd. Mihai Viteazul 1
Timisoara, Roumanie

1. Introduction

Turbulence is a property of the fluid flow rather than of the fluid itself. In a turbulent flow, the physical quantities, as well as the components of velocities and pressures, undergo fluctuations in time and space, permitting their being expressed by random variables. The turbulent diffusion, which is due to turbulent agitation, has effects exceeding the effects of molecular agitation, and thus causing the fast and intense mixture of the vortex tubes and the substantial amplification of the transfer of mass, momentum, moment of momentum, kinetic energy and heat through the boundary of an arbitrary control volume. Turbulence in the flow is the cause of the intense dissipation of kinetic energy into heat by the effect of viscosity [14, 15, 18, 20, 21, 29, 33, 36, 37, 42].

During the process of cavitation inception, turbulence may be a major factor, even a fundamental one. This means that, in defining and expressing the coefficient of cavitation inception, numerous physical quantities are involved, which define and generate turbulence. Thus, data on the field of turbulent pressures, the spectrum and the probable density are absolutely necessary. Also, in modelling the diffusion process, it is necessary to know the nuclei in the turbulent flow and the way in wich they respond to the temporal pressure fluctuations [19, 20].

2. The pressure in a turbulent flow

In the case of ideal fluid flow the tangential unit stresses are zero, while the normal stresses have a common value $(-p)$. The scalar quantity p is the pressure in a point of the domain filled by the moving ideal fluid.

FERZIGER [39] applied a convolution filter of the form

$$\bar{u}(\underline{r}) = \int G(|\underline{r} - \underline{r}'|)\, u(\underline{r}')\, \underline{dr}' \qquad (1)$$

to the Navier-Stokes [30] and continuity equations, in the case of incompressible fluids and homogeneous turbulent flow. In the Fourier space this becomes.

$$\hat{\bar{u}}(\underline{k}) = \hat{G}(k)\, \hat{u}(\underline{k}) \qquad (2)$$

if G is a function of k only. It follows that

$$\frac{\partial \bar{u}_i}{\partial t} + \frac{\partial}{\partial x_j}(\overline{u_i u_j}) = -\frac{1}{\rho}\frac{\partial \bar{p}}{\partial x_i} + \nu \frac{\partial^2 \bar{u}_i}{\partial x_j\, \partial x_j} \qquad (3)$$

and

$$\frac{\partial \bar{u}_i}{\partial x_i} = 0\,. \qquad (4)$$

But as

$$u_i = \bar{u}_i + u_i' \qquad (5)$$

it follows that

$$\overline{u_i u_j} = \overline{\bar{u}_i\, \bar{u}_j} + \overline{\bar{u}_i\, u_j'} + \overline{u_i'\, \bar{u}_j} + \overline{u_i'\, u_j'}\,. \qquad (6)$$

In equation (6)

$$R_{ij} = \overline{\bar{u}_i'\, \bar{u}_j} + \overline{\bar{u}_i\, u_j} + \overline{u_i'\, u_j'} \qquad (7)$$

is commonly called the subgrid scale (SGS) Reynolds stress.

The original method advenced by DEARDORFF [17] and extended by SCHUMANN [38] regarding the numerical solving of the equations (3) and (4) implies the simplifications

$$\overline{\bar{u}_i\, \bar{u}_j} = \bar{u}_i\, \bar{u}_j \qquad (8)$$

$$\bar{u}_i' = 0 \qquad (9)$$

which are properties this approach shares with Reynolds-averaged modelling. The subgrid scale Reynolds stress then reduce to

$$R_{ij} = \overline{u_i'\, u_j'}\,. \qquad (10)$$

The subgrid scale Reynolds stress defined by equation (7) can be decomposed into the sum of a trace-free tensor and a diagonal tensor

$$R_{ij} = \left(R_{ij} - \frac{1}{3}\,\delta_{ij}\,R_{kk} \right) + \frac{1}{3}\,\delta_{ij}\,R_{kk} \qquad (11)$$

or

$$R_{ij} = \tau_{ij} + \frac{1}{3}\,\delta_{ij}\,R_{kk}\,. \qquad (12)$$

When the decomposition (11) is substituted into the filtered Navier-Stokes equations (3), the diagonal component produces a term wich is equivalent to the gradient of a scalar. It is similar to the pressure gradient term and can be combined with it. It is therefore advantageous to define a modified pressure [19]

$$p^* = \bar{p} + \frac{\rho}{3}\,R_{kk}\,. \qquad (13)$$

The modified pressure p^* contains the whole spherical tension consisting of the static pressure, i.e. the mean pressure $\bar{p}$ of the non-viscous fluids in motion and the normal components of the Reynolds-stress tensor. In the case of isotropic turbulent motions ($\overline{u}_1'^2 = \overline{u}_2'^2 = \overline{u}_3'^2$) and of anisotropic turbulent motions ($\overline{u}_1'^2 \neq \overline{u}_2'^2 \neq \overline{u}_3'^2$) one has

$$R_{kk} = 3\,\overline{u}'^2 \qquad (14)$$

$$R_{kk} = \overline{u}_1'^2 + \overline{u}_2'^2 + \overline{u}_3'^2 = 3\,\overline{u}_a'^2\,. \qquad (15)$$

Cavitationally, the term $\rho/3\,R_{kk}$ expresses the negative peak of the pressure fluctuations in the turbulent flow.

3. Cavitation coefficients in flows with high degree of turbulence

At a point of the boundary layer flow in the vicinity of the solid wall, the dimensionless reserve of the relative pressure p^* with respect to the vaporisation pressure p_v of the working liquid (σ_{reserve}) is

$$\sigma_{\text{res}} = \frac{p^* - p_v}{\frac{1}{2}\rho U_\infty^2} = \frac{\bar{p} + \frac{1}{3}\rho R_{kk} - p_v}{\frac{1}{2}\rho U_\infty^2}$$

or

$$\sigma_{\text{res}} = \frac{p^* - p_v}{\frac{1}{2}\rho U_\infty^2} = \left[\frac{p_\infty - p_v}{\frac{1}{2}\rho U_\infty^2} \right] - \left[-\frac{\bar{p} - p_\infty}{\frac{1}{2}\rho U_\infty^2} - \frac{\frac{1}{3}\rho R_{kk}}{\frac{1}{2}\rho U_\infty^2} \right] \qquad (17)$$

$$\sigma_{\text{res}} = \frac{p^* - p_v}{\frac{1}{2}\rho U_\infty^2} = \left[\frac{p_\infty - p_v}{\frac{1}{2}\rho U_\infty^2} \right] - \left[-\frac{\bar{p} - p_\infty}{\frac{1}{2}\rho U_\infty^2} - \frac{\frac{1}{2}\rho R_{kk}}{\frac{1}{2}\rho U_e^2}\,\frac{U_e^2}{U_\infty^2} \right] \qquad (18)$$

where p_∞ and U_∞ represent the pressure and velocity of the umperturbed flow upstream from the tested plate, profile or body, and U_e is the velocity at the edge of the boundary layer in the vicinity of the wall,

$$C_p = \frac{\bar{p} - p_\infty}{\frac{1}{2}\rho U_\infty^2} = 1 - \left(\frac{U_e}{U_\infty} \right)^2 \qquad (19)$$

is the pressure coefficient at a point on the profile. If

$$\sigma_{\text{inst}} = \frac{p_\infty - p_v}{\frac{1}{2}\rho U_\infty^2} \qquad (20)$$

denotes the cavitation coefficient of the installation where the plate, profile or body to be tested is mounted [1, 3] and

$$\sigma = \left[-\frac{\bar{p} - p_\infty}{\frac{1}{2}\rho U_\infty^2} - \frac{\frac{1}{2}\rho R_{kk}}{\frac{1}{2}\rho U_e^2}\,\frac{U_e^2}{U_\infty^2} \right] = -C_p - (1 - C_p)\,\frac{\frac{1}{3}\rho R_{kk}}{\frac{1}{2}\rho U_e^2} \qquad (21)$$

the cavitation coefficient σ of the body over which a viscous liquid flow [1, 3] then

$$\sigma_{\text{res}} = \frac{p^* - p_v}{\frac{1}{2}\rho U_\infty^2} = \sigma_{\text{inst}} - \sigma\,. \qquad (22)$$

If, at a certain moment, the modified pressure p^* at some point of the liquid flow decreases to the vaporization pressure ($p^* = p_{\min} = p_v$) i.e. to its minimum value, the inception of cavitation ($\sigma_{\text{res}} = 0$) occurs.

At this moment the coefficients of cavitation are equal in value, differing in their physical signification and expression [1, 3].

$$\sigma_i = \frac{p_\infty - p_v}{\frac{1}{2}\rho U_\infty^2} = -C_{p\,\min} - (1 - C_{p\,\min})\,\frac{\frac{1}{3}\rho R_{kk}}{\frac{1}{2}\rho U_e^2}\,. \qquad (23)$$

Consequently

$$\sigma_i = -C_{p\,\min} + \Delta\sigma_T \qquad (24)$$

where

$$\Delta\sigma_T = -(1 - C_{p\,\min})\,\frac{\frac{1}{3}\rho R_{kk}}{\frac{1}{2}\rho U_e^2} \qquad (25)$$

represents the effect of turbulence on the coefficient of cavitation inception. In order to know the effect of turbulence $\Delta\sigma_T$ on the cavitation coefficient σ_i and on the cavitation curves [3] it is necessary to determine R_{kk} i.e., the pressure fluctuations in the turbulent flow.

4. Pressure fluctuations in turbulent flows

The problem of pressure fluctuations was considered both theoretically and experimentally. The effective (rms) pressure coefficient of pressure fluctuations is given in *figure 1* for the case of cylindrical body in the current, as measured by THARA and MURAI [24]. Here

$$C'_{p\,\mathrm{rms}} = 2\,\bar{p}'/\rho U_\infty^2 \tag{26}$$

where

$$\bar{p}' = \left[\sum_{n=1}^{N} x_n^2/(N-1)\right]^{1/2} \tag{27}$$

$$x_n = p_n - \bar{p} \tag{28}$$

$$\bar{p} = \left(\sum_{n=1}^{N} p_n\right)/N \tag{29}$$

N being the number of measurements.

The computational determination of R_{kk} is an extremely complex problem, whose starting point is the Navier-Stokes equation [9, 10, 12, 19, 36, 37, 40, 41] ;

$$\frac{\partial u_i}{\partial t} + \frac{\partial}{\partial x_i} u_i\, u_j = -\frac{1}{\rho}\frac{\partial p}{\partial x_i} + \nu \frac{\partial^2 u_i}{\partial x_j\, \partial x_j}\,. \tag{30}$$

If the divergence is applied to this equation, there result

$$\nabla_p^2 \equiv \frac{\partial^2 p}{\partial x_i\, \partial x_i} = -\rho \quad \frac{\partial^2 (u_i\, u_j)}{\partial x_i\, \partial x_j} = Q(x, t) \tag{31}$$

a second degree Poisson equation.

The pressure fluctuation as a function of the velocity field results from Poisson equation by decomposing the variables into mean and fluctuating values. In this case

$$\frac{\partial^2 p'}{\partial x_i\, \partial x_i} = -2\,\rho \frac{\partial \bar{u}_i}{\partial x_j}\frac{\partial u'_j}{\partial x_i} - \rho \frac{\partial^2}{\partial x_i\, \partial x_j}(u'_i\, u'_j - \overline{u'_i\, u'_j}) = -\rho\sigma\,. \tag{32}$$

The first term on the righ-hand side of this equation represents the turbulence and mean-shear interaction, while the second term represents the turbulence-turbulence interaction. For a wall-boundary flow, if contributions from surface integrals are neglected, the fluctuating pressure at a point X on the wall is given by [39]

$$p'(x) = \frac{\rho}{2\,\pi}\int_{y>0} \frac{\sigma(R_s)\, dV(R_s)}{(x - R_s)} \tag{33}$$

where the volume V integration is at position R_s over the entire halfspace containing the flow. Equation (33) shows that the pressure fluctuations are generated by sources in the whole domain of the flow, but the contribution of the different sources decreases rapidly with the distance from the point taken into consideration.

BATCHELOR [9, 10] was the first to determine the mean-square fluctuation for the isotropic turbulent flow and he obtained

$$\overline{[p'^2]}^{1/2} = k_1 \frac{\rho}{2}\,\bar{u}'^2 \tag{34}$$

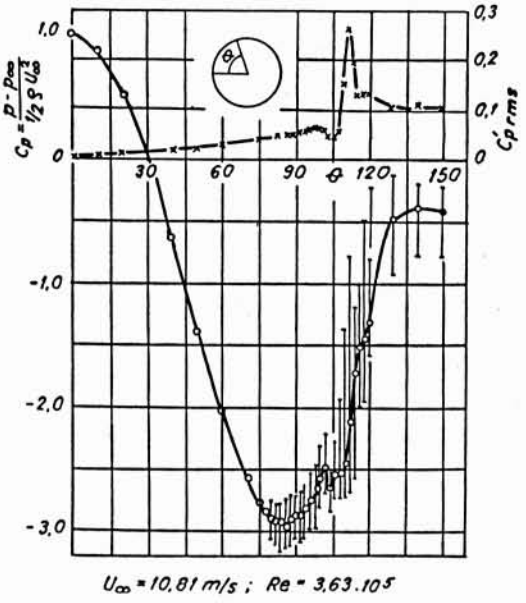

1. *Pressure distribution on the cylinder.*

where

$$k_1 = 1.2 - 1.4\,.$$

In this case

$$\frac{\rho}{3} R_{kk} = \frac{2}{k_1}\overline{[p'^2]}^{1/2} = k_p\,\overline{[p'^2]}^{1/2} \tag{35}$$

where $k_p = 1.66 \div 1.42$.

UBEROI [43] confirmed this result experimentally utilising the hot wire technique, and he obtained

$$k_1 \cong 1.4\,.$$

KRAICHNAN [26, 27] gave more general solutions of equation (33), for both cases of the anisotropic turbulent field and for that of the isotropic field. By simplification, these solutions can be expressed in the following form

$$\frac{\overline{[p'^2]}^{1/2}}{\frac{1}{2}\rho U_e^2} = k_2 \frac{\overline{u_1'^2}}{U_e^2}, \quad \text{where} \quad \begin{cases} k_2 \cong 1.4 \text{ isotropic flow} \\ k_2 > 1.4 \text{ shear flow}\,. \end{cases} \tag{36}$$

For the pressure fluctuation at the wall, KRAICHNAN [27] obtained

$$\overline{[p'^2]}^{1/2} = 6\,\tau_w = k_w\,\tau_w \tag{37}$$

where τ_w is the mean shear stress at the boundary surface, which can be expressed as a function of the friction

velocity U_τ or of the skin friction coefficient C_f [22] knowing that

$$\tau_w = \rho U_\tau^2 \tag{38}$$

$$C_f \frac{\tau_w}{\frac{\rho}{2} U_e^2} = 2 \frac{U_\tau^2}{U_e^2} \quad \text{for boundary layers} \tag{39}$$

$$C_f = \frac{\overline{u_1' u_2'}}{U_e^2} \quad \text{for jets and wakes .} \tag{40}$$

ARNDT [8] showed that numerous studies indicated the value 2.8 for k_w. FAVRE [18] considered that $k_w = 2.2 - 2.8$ and that it increased with the Reynolds number. WILLMARTH [44-46] obtained $k_w = 2 - 3$ by laboratory measurements, while MC GRATH and SIMPSON [39] obtained 2.3. More recent theoretical and experimental studies [4, 23, 25, 28, 30, 34, 35] provide numerous results regarding the velocity of pressure fluctuations within the boundary layer, which permit the approximate computation of the term $\rho/3\, R_{kk}$, in the expression of the modified pressure and, consequently, of the cavitation coefficient σ_i.

KIM *et al.* [25] numerically solved the Navier Stokes equations for the homogeneous turbulent motion in a channel. The computation was carried out with 3.962.880 grid points ($192 \times 129 \times 160$ in x, y, z) for a Reynolds number of 3.300, with is based on the mean centre line velocity and the channel half-width.

The computed values of the velocity fluctuations wich were given as root-mean-square velocity fluctuations normalized by the well shear velocity

$$u'_{1\,\mathrm{rms}} = \frac{\overline{[u_1'^2]}^{1/2}}{U_\tau}; \quad u'_{2\,\mathrm{rms}} = \frac{\overline{[u_2'^2]}^{1/2}}{U_\tau};$$

$$u'_{3\,\mathrm{rms}} = \frac{\overline{[u_3'^2]}^{1/2}}{U_\tau};$$

fully agree with the measured values of KREPLIN and ECKELMANN [28].

Assuming that the rms of R_{kk} is

$$\frac{R_{kk}}{U_\tau^2} = u'^2_{1\,\mathrm{rms}} + u'^2_{2\,\mathrm{rms}} + u'^2_{3\,\mathrm{rms}} = 3\, u'^2_{a\,\mathrm{rms}} \tag{41}$$

then

$$\frac{1}{3} \frac{R_{kk}}{U_\tau^2} = u'^2_{a\,\mathrm{rms}} = k_R . \tag{42}$$

The values of the coefficient k_R computed by KIM *et al.* [25], MOSER *et al.* [30] and those measured by KREPLIN *et al.* [28] for the turbulent flow with small Reynolds number are shown in *table 1* for different values of $y^+ = \frac{yU_\tau}{\nu}$.

KIM *et al.* [25] also computed the root-mean-square (rms) pressure normalized by shear velocity (*fig. 2*).

PERRY, LIM and HENFEST [35] experimentally determined the velocity fluctuations in the boundary layer at different distances y/δ from a smooth wall. The values of k_R are given in *table 2*.

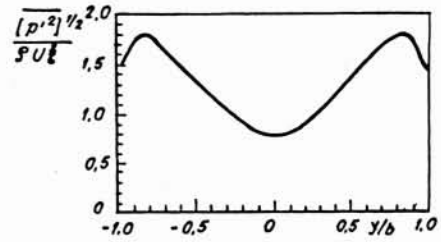

2. *Root-mean-square pressure fluctuation normalized by the wall shear velocity.*

The results given in the foregoing refer to the turbulent flow in a channel or over a smooth plate at small Reynolds numbers, when no detachment from the wall occurs. However, as hydraulic machines operate under conditions differing from the optim ones, wich means that when the flow passes over the runner blades it displays a separating boundary layer, it is interesting to analyse the turbulent flow detached from the wall.

PANTON and LINEBARGER [34] calculated wall pressure spectra for-zero-pressure-gradient and adverse pressure-gradient equilibrium boundary layers that seem to describe, the essential features observed from experiments. They used Coles'lawn of the wall and wake for mean velocity profiles. A scale anisotropic model of the spatial correlation of $u_2'^2$ was used together with the assumption that $u_2'^2$ was proportional to $(-\overline{u}_1', \overline{u}_2')$ for all equilibrium layers and thus they obtained the coefficient $k_w = f(\mathrm{Re}, \Pi, \alpha)$ (*tabl. 3*).

Hence it follows that the flow with boundary layers without separation and consequently with small pressure gradient $k_w = 2.89 - 3$ while for the flow with adverse-pressure-gradient equilibrium and separating turbulent boundary layers $k_w = 4.40 - 19.87$ and $k_M = 1.4 - 2.07$.

SIMPSON *et al.* obtained the same result by analysing the theoretical findings of PANTON and LINEBARGER [34], as well as some experimental data regarding the surface pressure fluctuations in a separating turbulent boundary layer, wich are shown in *table 4*.

Thus $k_w = 4.09 - 11.44$ and $k_M = 1.20 - 2.75$. For the computation of the pressure fluctuations at the wall, SIMPSON *et al.* [39] gave the equation

$$\overline{[p'^2]}/\tau_w^2 = 0.52\, \alpha^{0.9} \left(\ln \left| \frac{u_\tau \delta}{\nu} \right| + 9.24 \right) \tag{43}$$

which agrees with the computations of PANTON and LINEBARGER [34] for the zero-pressure gradient with $\alpha = 1$; 2 and 3 and COLES wake function parameter $\Pi = 0.6$. Here the Reynolds number is in terms of the displacement-thickness Reynolds number

$$\frac{u_\tau \delta}{\nu} = \frac{k}{1 + \Pi} \left(\frac{U_\infty \delta^*}{\nu} - 65 \right) \tag{44}$$

where $k = 0.41$ (COLES and HIRST [16]).

Table 1

y^+	10	20	30	40	60
k_{Rt}	2,41	2,53	2,06	1,72	1,54
k_{Rexp}	2,85	2,65	1,99	1,91	1,66

Table 2

y/δ	0.01	0,05	0,1	0,5
$k_R = \frac{1}{3}\frac{R_{kk}}{U_\tau^2}$	3,2	2,8	2,7	1,26

Table 3

$Re = \frac{U_\tau \delta}{\nu}$	1000	4000	10000	4000	4000	400	4000	4000	4000
Π	0,6	0,6	0,6	1,5	3	6	0,6	6	3
α	1	1	1	1	1	1	2	3	2
$k_w = \frac{[\overline{p'^2}]^{1/2}}{\tau_w}$	2,89	3,01	3,10	4,37	7,89	6,28	4,15	4,92	11,40
$k_M = \frac{[\overline{p'^2}]^{1/2}}{\tau_M}$	-	-	-	1,61	1,43	1,40	-	-	2,07

Table 4

No.	Re_δ 10^{-3}	U_τ/U_∞	Π	H	U_M/U_∞	$k_w = \frac{[\overline{p'^2}]^{1/2}}{\tau_w}$	$k_M = \frac{[\overline{p'^2}]^{1/2}}{\tau_M}$
1. Bradshaw (1967) equilibrium	40,3	0,0252	2,9	1,59	0,0566	8,83	1,84
2. Lim (1971) equilibrium	28,4	0,0291	1,92	1,56	0,1546	4,09	1,23
	32,4	0,0294	1,92	1,52	0,0519	4,33	1,31
3. Scloner (1967) non-equilibrium	14,6	0,0296	1,84	1,56	0,0563	4,34	1,2
4. Hahn (1976) airfoil	38	0,021	4,7	2,33	0,060	11,44	1,40
	48	0,030	0,9	1,33	0,038	4,42	2,73
5. Burton (1973) non-equilibrium	-	0,023	-	1,76	0,059	9,59	1,45
6. Călin (1988) airfoil NACA 4412	5,08	0,0316	2,29	1,624	0,0419	3,9	2,22

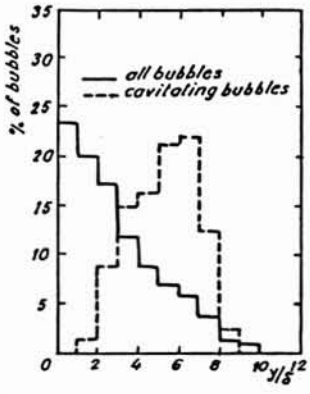

3. *Distribution of gas bubbles in the boundary layer flow.*

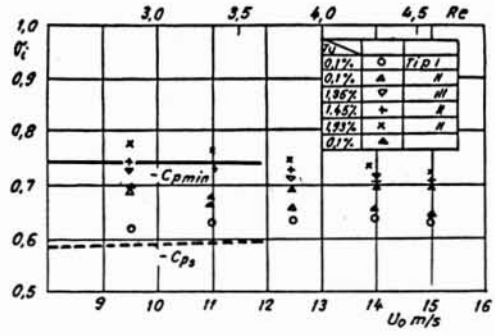

4. *Correlation of cavitation data for turbulent flow.*

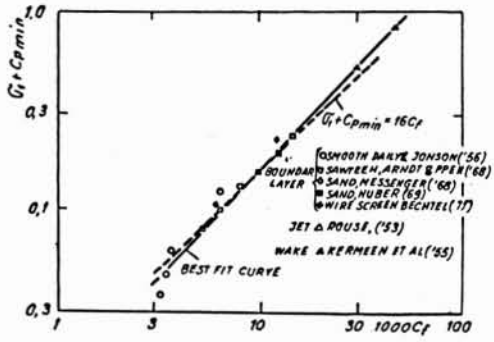

5. *Variation of the cavitation coefficient σ_i with the velocity and turbulence degree on the JTTC body.*

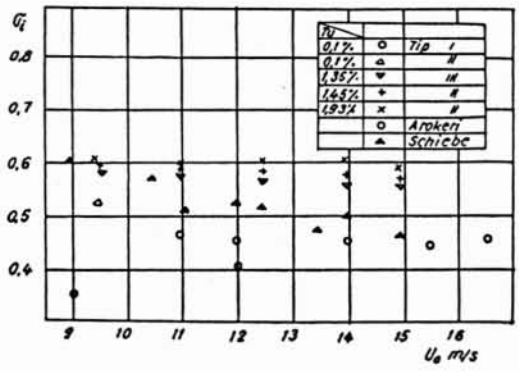

6. *Variation of the cavitation coefficient σ_i with the velocity and turbulence degree on the JTTC body.*

SIMPSON *et al.* [39] showed that the local maximum shearing stress τ_M (wich occurs in the middle of the boundary layer) appears to be the proper stress on which to scale $\overline{[p'^2]}^{1/2}$; from available data

$$\overline{[p'^2]}^{1/2}/\tau_M = k_M \qquad (45)$$

shows less variation than when $\overline{[p'^2]}^{1/2}$ is scaled on the wall shear stress τ_w, for the flow with small pressure gradients and with pressure of adverse pressure gradients and separation boundary layers. SIMPSON *et al.* [39] determined a relation for τ_M as a function of the shape parameter H

$$\frac{\tau_M}{\frac{1}{2}\rho U_e^2} = \left[\frac{1}{6.55}\left(1-\frac{1}{H}\right)\right]^2. \qquad (46)$$

In the measurements made by SIMPSON *et al.* [39] both the turbulence and mean-shear interaction and turbulence--turbulence interaction in the pressure fluctuation source term (32) are important for detached flows.

Velocity fluctuations are as large as mean velocity in the back flow Reynolds shear stress and their gradients are large, away from the wall. Thus the largest pressure fluctuations are not at the wall in a detached flow but must be near the middle of shear layer.

From a cavitational point of view this is a very important conclusion, as ARNDT and IPPEN [4, 6] concluded from observations made on the growth of bubbles in the boundary layer as would be expected from the observation that the peak in the wall pressure spectrum is due to fluctuations in this region.

In *figure 3* a histogram is presented, which was obtained by ARNDT and IPPEN [5] who measured the frequency of cavitation incipience for approximatively 8.000 bubbles. The full line correspond to the distribution of bubbles which do not expand, while the dotted line gives the distribution of expanding bubbles. In all the cases studied by ARNDT and IPPEN the highest frequency of cavitational incipience occurred at an approx. (0.4-0.5) δ from the solid wall. ARNDT and IPPEN [5, 6, 8] consider that the only explication for the localization of cavitation incipience at the middle of the boundary layer is the fact that the minimum of pressure fluctuations appears in this zone.

5. Relations for the cavitational scale. Effect due to turbulence

It follows from relations (15) and (25) that the effect of turbulence on the cavitation coefficient $\Delta\sigma_T$ may be expressed as

$$\Delta\sigma_T = (1 - C_{p\,\min})\, 2\, \frac{\overline{u}'^2}{U_e^2} \quad \text{(isotropic flow)} \quad (47)$$

$$\Delta\sigma_T = (1 - C_{p\,\min})\, 2\, \frac{u_a'^2}{U_e^2} \quad \text{(anisotropic flow)} \quad (48)$$

and from relations (25), (39) and (42) that

$$\Delta\sigma_T = (1 - C_{p\,\min})\, \frac{k_R\, \tau_w}{\rho/2\, U_e^2} = (1 - C_{p\,\min})\, k_R\, 2\, \frac{U_\tau^2}{U_e^2} \quad (49)$$

or

$$\Delta\sigma_T = (1 - C_{p\,\min})\, k_R\, C_f = C_1\, C_f\,. \quad (50)$$

Figure 4, from ARNDT [5, 8] gives the cavitation data obtained in boundary layers, jets and wakes.

The skin friction coefficient C_f is computed either form measured wall shear stress or form measurements made in air at comparable Reynolds number for the cases of a free jet and wake

$$C_1 = (1 - C_{p\,\min})\, k_R \cong 16 \quad (51)$$

and appears to be a good approximation of these data.

NAGANO *et al.* [32] determined the coefficient C_f for a flat plate boundary relaminirizing flow and diffuser flow.

Using the local maximum shearing stress τ_M in relation (25), (35), (45), (46) it follows that

$$\Delta\sigma_T = (1 - C_{p\,\min})\, k_p\, k_M\, \frac{\tau_M}{\frac{1}{2}\rho U_e^2} \quad (52)$$

and

$$\Delta\sigma_T = (1 - C_{p\,\min})\, k_p\, k_M \left[\frac{1}{6.55}\left(1 - \frac{1}{H}\right)\right]^2. \quad (53)$$

Relations (47)-(53) seem to have completely clarified and solved the problem, as they express, in various forms, the cavitation scale effect caused by turbulence. In fact, the problem is not so simple and requires further theoretical and experimental research. The turbulence level may affect the value of the cavitation inception coefficient in two ways : first, by the direct reduction of the local static pressure by the turbulent pressure fluctuations and second, by the growth of the gas bubble under the conditions of the rectified gas diffusion.

MURAI and IHARA [31] showed that if the turbulent pressure fluctuations were dominant, the constant k_1 in (34) corresponded to the values computed by BATCHELOR [9] and measured by UBEROI [43]. The experimental value obtained by MURAI and IHARA [31] in velocity field of 12 m/sec., without measuring the air content, was about 140 times higher than that obtained UBEROI.

This great difference is explained by the fact that the dominant process in the water flow displaying cavitation is the growth of the free-gas nuclei in the flow, rectified diffusion being present. By way of illustration, the experimental results obtained on a hemispherical-nosed body and on the ITTC standard body are shown in *figures 5 and 6* respectively. These results point out the influence of the turbulence level on the incipient of cavitation. It should be noted that I corresponds to the inception of the strip-type or attached-sheet-type cavitation and II to the travelling-cavitation bubble appearing away from the wall of the body and cavitating close to the point $C_{p\,\min}$.

Figure 7 from MURAI and IHARA [31] shows the influence of the turbulence level for different bodies of simple geometry.

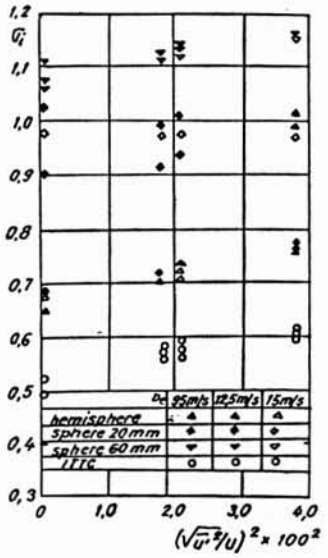

7. *Influence of turbulence on the cavitation on the inception coefficient* σ_i.

6. Conclusions

Turbulence strongly influences the coefficients of cavitation incipience σ_i in a direct way, through the pressure fluctuation, and also indirectly due to the intensification of rectified gas diffusion in the cavitating bubble. The relations established in the present work to exprime the scale effect $\Delta\sigma_T$ due to turbulence, are based on the idea that the maximum pressure fluctuations produced by turbulence occurs at a distance from the wall, in particular in the middle part of the boundary layer, attached or detached. The effects of rectified diffusion in the conditions of turbulence were neglected.

The above results concerning the cavitation incipience scale effects due to turbulence, represent a step forward in understanding this complex problems, which need further theoretical and experimental investigations.

References

[1] ANTON I., Curbe caracteristice de cavitaţie teotice şi experimentale la pompele centrifuge de turaţie specifică joasă. *St. cerc. şt. Acad. RSR Timişoara,* Tom 7(3-4), 1960, pp. 62-100.

[2] ANTON I., *Turbine hidraulice,* Ed. Facla Timişoara 1979.

[3] ANTON I., *Cavitaţia* I, II, Ed. Acad. RSR, 1984-85.

[4] ARAKERI H.V., ACOSTA A., Viscous effects in the inception of cavitation, *ASME,* 1981, 103, 519-526.

[5] ARNDT R.E.A., IPPEN A.T., Rough surface effects on cavitation inception, *J. Basic. Eng.,* 1968, 90, 249-261.

[6] ARNDT R.E.A., DAILY J.W., Cavitation in turbulent boundary layers. *Proc. Symp. Cavitation State Knowledge ASME,* Evanston Illinois 1969, 64-36.

[7] ARNDT R.E.A., Pressure fields and cavitation. *7th Symp. AIRN,* Vienne 1974.

[8] ARNDT R.E.A., Recent advances in cavitation research, in *Advances in Hydroscience,* 1981, 12.

[9] BATCHELOR K.G., Pressure fluctuation in isotropic turbulence, *Proc. of the Cambridge Phil. Soc.* 1951, 47, 2.

[10] BATCHELOR K.G., *The theory of homogeneous turbulence.* Cambridge Univ. Press. 1960.

[11] BRADSHAW F., *An introduction to turbulence and its measurements.* Pergamon Press, Oxford 1971.

[12] BRADSHAW P., CEBECI T., *Engineering calculation methods for turbulent flow.* Acad. Press. London 1981.

[13] CĂLIN Gh., *Studiul curgerii vîscoase printr-o reţea plană de profile.* Teză de doctorat, I.P. Timişoara, 1988.

[14] CLAUSER H.F., Turbulent boundary layers in adverse pressure gradients, *Jour. Aero. Sci.* 1954, 21, 91-108.

[15] COLES E.D., The law of the wake in turbulent boundary layer. *J. Fluid Mech.* 1956, 1, 191-226.

[16] COLES E.D., HIRST E., *Computational of turbulent boundary layers,* Stanford Univ. 1969.

[17] DEARDORFF J., A numerical study of three-dimensional turbulent channel flow at large Reynolds numbers. *J. Fluid Mech.* 1970, 41, 2, 453-480.

[18] FAVRE A., KOVASZNAY L., DUNCA R., GAVIGLIC J., COARATIE U., *La turbulence en mécanique des fluides,* Gauthier-Villars, Paris, 1976.

[19] FERZIGER J.H., *Higher-Level simulations of turbulent flows. Computational methods for turbulent, transsonic and viscous flows,* Springer Verlag, 1983.

[20] HINZE J.C., *Turbulence,* Mc Graw-Hill, 1975.

[21] HOLL J.W., BILLET L.M., TADA M., The influence of pressure gradient on desinent cavitation from isolated surface protrusions. *ASME J. Fluid Eng.* 1986, 108, 254-260.

[22] HONDA M., IGARASHI S., An analysis of turbulent boundary layer flow without pressure gradients. *Rep. Inst. High Speed Mech.* Tohonu Univ. 1976, 33, p. 1, 2.

[23] HUANG T.T., Cavitation inception observations on six axisymmetric head forms, *ASME J. Fluids Eng.* 1981, 103, 273-279.

[24] IHARA A., MURAI H., Cavitation inception on a circular cylinder at critical and supercritical flow range. *ASME J. Fluids Eng.* 1986, 108, 421-427.

[25] KIM J., MOIN P., MOSER R., Turbulence statistics in fully developed channel flow at low Reynolds number, *J. Fluid Mech.* 1989, 177, 133-166.

[26] KRAICHNAN R.H., Pressure field within homogeneous anisotropic turbulence. *J. Acoust. Soc. Am.* 1956, 28, 1, 64-74.

[27] KRAICHNAN R.H., Pressure fluctuations in turbulent flow over a flat plate. *J. Acoust. Soc. Am.,* 1956, 28, 3, 378-390.

[28] KREPLIN H.V., ECKELMANN H., Behaviour of the three fluctuating velocity components in the wall region of a turbulent channel flow. *Phys. Fluids.* 1979, 22, 7, 1233-1239.

[29] LUDVIEG H., TILLMAN W., Untersuchungen Über die Wandschubspannung in turbulenten Reibungsschichten. *Ing. Arch.* 1949, 17, 288-299.

[30] MOSER R., MOIN P., The effects of curvature in wall-bounded turbulent flow, *J. Fluid Mech.* 1987, 175, 479-510.

[31] MURAI H., IHARA A., Effects of free stream turbulence and free stream velocity on cavitation inception of axisymmetric bodies. *Rep. Inst. High. Speed. Mech. Tohoku Univ.* 1980, 42, 101-127.

[32] NAGANO Y., HISHIDA M., Improved form of the K- model for wall turbulent shear flows. ASME, *J. Fluids Eng.* 1987, 109, 156-160.

[33] NASH F.J., *Turbulent-boundary-layer. Behaviour and the auxiliary equation.* Nat. Phys. Lab. Aero. Rep. 1135, 1965.

[34] PANTON R.L., LINEBARGER J.H., Wall pressure spectra calculations for equilibrium boundary layer. *J. Fluid Mech.* 1974, 65, 261-287.

[35] PERRY A.E., LIM H.L., HENBEST S.M., An experimental study of the turbulence structure in smooth- and rough-wall boundary layers. *J. Fluid Mech.* 1987, 177, 437-466.

[36] POPA O., *Mecanica fluidelor şi măsuri hidraulcie. I.* P. Timişoara, 1980.

[37] SCHLICHTING N., *Boundary layer theory.* Mc Graw-Hill Book, New York, 1960.

[38] SCHUMANN U., *Ein verfahren zur direkten numerischen Simulation turbulent Strömungen in Platten und Ringapaltkanalen and über seine Anwendung zur Untersuchung von Turbulenzmodellen.* Disc. Univ. Karlsruhe, 1973.

[39] SIMPSON R.L., GHODBANE M., MC GRATH B.E., Surface pressure fluctuations in separating turbulent boundary layer, *J. Fluid. Mech.,* 1987, 177, 167-186.

[40] TENNEKES N., LUMLEY J. L., *A first course in turbulence,* The MTT Press. Masachusetts, 1972.

[41] TOWNSEND A., *The structure of turbulent shear flow,* Cambridge Univ. Press. 1966.

[42] TRUCKENBRODT E., Ein Quadraturverfahren zur Berechnung von Strömungsgrenzschichten mittels einfacher Quadraturformeln. *Ing. Arch.* Theil I, 1973, 43, 9.

[43] UBEROI M.S., *Correlations involving pressure fluctuations in homogeneous turbulence.* NACA, Tech. Note 3116 (1954).

[44] WILLMARTH W.W., Pressure fluctuations beneath turbulent, *Am. Rev. Fluid Mech.,* 1975, 7, 13-38.

[45] WILLMARTH W.W., *Structure of turbulence boundary layers,* Advances Appl. Mech., Academic Press New York, 1959, 15.

[46] WOOLDRIGE C.E., WILLMARTH W.W., *T.R. Umich,* ORA Pr. 02920, Ann Arbor, 1962.